Electronic Supplementary Material (ESI) for Chemical Communications.
This journal is © The Royal Society of Chemistry 2020

Electronic Supplementary Information (ESI)

Solvent Vapor-Induced Polarity and Ferroelectricity Switching

Fumiya Kobayashi[a], Ryohei Akiyoshi[b], Daisuke Kosumi[c,e], Masaaki Nakamura[b], Leonard F. Lindoy[d] and Shinya Hayami*[,b,e]

[a] Department of Chemistry, Faculty of Science, Tokyo University of Science, 1-3 Kagurazaka, Shinjuku-ku, Tokyo 162-8601, Japan.

[b] Department of Chemistry, Graduate School of Science and Technology, Kumamoto University, 2-39-1 Kurokami, Chuo-ku, Kumamoto 860-8555, Japan.

[c] Department of Physics, Graduate School of Science and Technology, Kumamoto University, 2-39-1 Kurokami, Chuo-ku, Kumamoto 860-8555 Japan.

[d] School of Chemistry, the University of Sydney, NSW 2006, Australia.

[e] Institute of Industrial Nanomaterials (IINa), Kumamoto University, 2-39-1 Kurokami, Chuo-ku, Kumamoto 860-8555, Japan.

Corresponding author:

S. Hayami, hayami@kumamoto-u.ac.jp

Experimental Section

General

All reagents and solvents were obtained from Tokyo Kasei Co. and Wako Pure Chemical Industries and were of reagent grade; they were used without further purification. All reactions were carried out under ambient atmosphere.

Synthesis

Preparation of H_2sap ligand

o-Aminophenol (0.55 g, 5 mmol) was added to salicylaldehyde (0.61 g, 5 mmol) in MeOH (50 mL) and the solution was refluxed for 2 h. On allowing the solution to stand, H_2sap was obtained as orange crystals. Yield: 0.853 g (80%). Anal. Calc. for $C_{13}H_{11}NO_2$: C, 73.23; H, 5.20; N, 6.57. Found: C, 73.20; H, 5.32; N, 6.43%.

*[Fe(sap)(acac)(MeOH)] (**1**)*

A methanol solution (10 mL) of $Fe(acac)_3$ (0.353 g, 1.00 mmol) was added with stirring to H_2sap (0.213 g, 1.00 mmol) in methanol (30 mL) and stirring was continued for 3 h at 80°C in air. On cooling the solution to room temperature, **1** was obtained as a brown powder which was dissolved in MeOH and the solution was allowed to stand for a few days during which time black block crystals formed. They were collected by suction filtration, washed with small amount of cold methanol, and dried in air. Yield: 0.239 g (60%). Anal. Calc. for **1** ($C_{19}H_{20}NFeO_5$): C, 57.31; H, 5.06; N, 3.52. Found: C, 57.58; H, 5.22; N, 3.63%.

*[Fe(sap)(acac)(DMSO)] (**2**)*

Complex **2** was obtained by dissolving **1** in MeOH/CH_2Cl_2/DMSO (2:2:1) and allowing the solution to stand for a few days. During this time black quartz-like (**2a**) and block type (**2b**) crystals formed. However, when **1** was recrystallized solely from DMSO, only the block type (**2b**) crystals were obtained. Anal. Calc. for **2** ($C_{20}H_{22}NFeSO_5$): C, 54.07; H, 4.99; N, 3.15. Found: C, 54.32; H, 5.03; N, 3.25%.

*[Fe(sap)(acac)(py)]·0.5py (**3**)*

Complex **3** was prepared by dissolving **1** in a MeOH/pyridine mixture (1:1) and allowing the solution to stand for a few days, during which time black block type crystals formed. Anal. Calc. for **3** ($C_{25.5}H_{23.5}N_{2.5}FeO_4$): C, 63.17; H, 4.89; N, 7.22. Found: C, 63.10; H, 5.11; N, 7.05%.

Solvent vapor exchange experiments

A small amount (ca. 2 mg) of the ground crystalline sample chosen from **1**−**3** was added to a small glass vial. The vial was placed in a larger capped glass vial together with a small amount of the required solvent (MeOH, DMSO or pyridine, ca. 2 mL) as the vapor source. The sealed system was left to stand for 1−5 days at room temperature (ca. 25 °C).

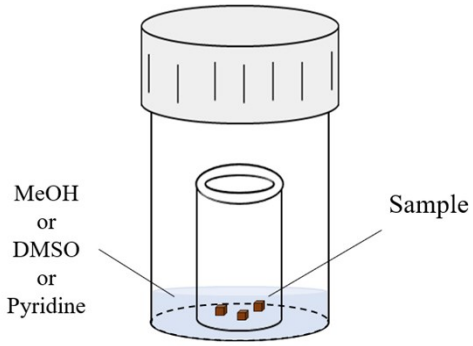

Physical Measurements

Elemental analyses

Elemental analyses (C, H, N) were carried out at the Instrumental Analysis Centre of Kumamoto University. Infrared (IR) spectra measurements were performed on a PerkinElmer Spectrum Two FT-IR equipped with an ATR accessory.

Single crystal X-ray diffraction

The single crystal X-ray diffraction data for **1**–**3** was recorded on a Rigaku XtaLAB mini II diffractometer employing graphite monochromated Mo Kα radiation generated from a sealed tube (λ = 0.7107 Å). Data integration and reduction were undertaken with CrysAlisPro. Using Crystal Structure software, the structure was solved with the SHELXT structure solution program using Direct Methods and refined with the SHELXL refinement package using Least Squares minimization. Hydrogen atoms were included in idealized positions and refined using a riding model. Powder X-ray diffraction data (PXRD) were collected on a Rigaku MiniFlex II ultra (30 kV/15 mA) X-ray diffractometer using Cu Kα radiation (λ = 1.5406 Å) in the 2θ range of 5°−30° with a step width of 1.0°.

Dielectric property measurements

Temperature-dependent dielectric constants in the frequency range 10–100000 Hz were measured using an inductance capacitance and resistance (LCR) meter on a Wayne Kerr 6440B LCR meter. The determination of polarization was performed on an aixACT TF analyzer 1000.

Table S1. Crystallographic data for **1**, **2a**, **2b** and **3**.

Compound	**1**	**2a**	**2b**	**3**
T / K	123	298	298	298
Crystal system	Triclinic	Monoclinic	Monoclinic	Monoclinic
Space group	*P*-1 (#2)	*Cc* (#9)	*Cc* (#9)	$P2_1/n$ (#15)
a / Å	9.678(6)	18.1583(10)	16.110(6)	9.3051(19)
b / Å	11.053(6)	17.6762(5)	19.650(4)	19.938(3)
c / Å	17.646(11)	8.0886(5)	8.238(5)	12.331(2)
α / °	92.405(7)	90	90	90
β / °	103.003(12)	128.002(9)	125.84(5)	111.89(2)
γ / °	99.572(12)	90	90	90
V / Å^3	1807.3(19)	2045.8(3)	2114.1(18)	2133.0(7)
Z	4	4	4	4
D_{calc} / g cm^{-3}	1.467	1.442	1.396	1.510
μ / mm^{-1}	0.863	0.870	0.841	0.746
R1	0.0713	0.0235	0.0802	0.0506
wR2	0.1355	0.0630	0.2660	0.1708
Flack	—	0.009(10)	-0.003(8)	—
CCDC	—*	1996715	—*	1996716

*The crystal structures for **1** and **2b** are in accord with those of reported compound.[S1,2]

[S1] T. Nakamura, E. Kuranuki, K. Niwa, M. Fujiwara, T. Matsushita, *Chem. Lett.* **2000**, *29*, 248–249.

[S2] M. Bagherzadeh, L. Tahsini, R. Latifi, V. Amani, A. Ellern, L. K. Woob, *Inorg. Chem. Commun*. **2009**, *12*, 476–480.

Table S2. Selected bond lengths (Å) and angles (°) for **1**, **2a**, **2b** and **3**.

Compound	**1** (123 K)	**2a** (298 K)	**2b** (298 K)	**3** (298 K)
Fe1–N1	2.127(4)	2.165(4)	2.170(1)	2.049(9)
Fe1–O1	2.000(3)	1.926(2)	1.907(1)	1.848(3)
Fe1–O2	1.916(3)	1.963(2)	1.974(1)	1.870(2)
Fe1–O3	1.966(3)	1.990(1)	2.018(9)	1.897(2)
Fe1–O4	2.025(3)	2.034(2)	2.035(1)	1.931(3)
Fe1–O5	2.087(3)	2.063(2)	2.063(1)	—
Fe1–N2	—	—	—	2.124(3)
Fe2–N2	2.123(4)			
Fe2–O6	2.006(3)			
Fe2–O7	1.917(3)			
Fe2–O8	1.970(3)			
Fe2–O9	2.023(3)			
Fe2–O10	2.083(3)			

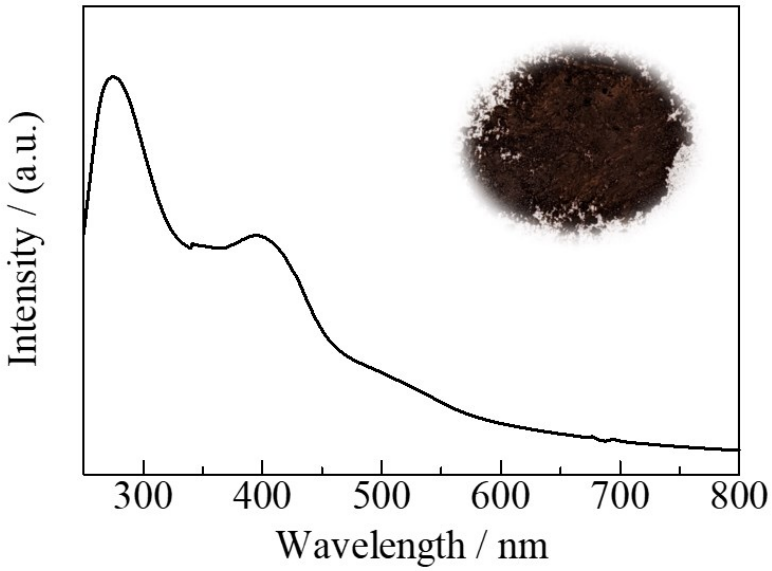

Figure S1. UV-vis absorption spectrum (λ_{abs} = 276, 396 nm) for **1** (inset; brown powder) in the solid state at room temperature.

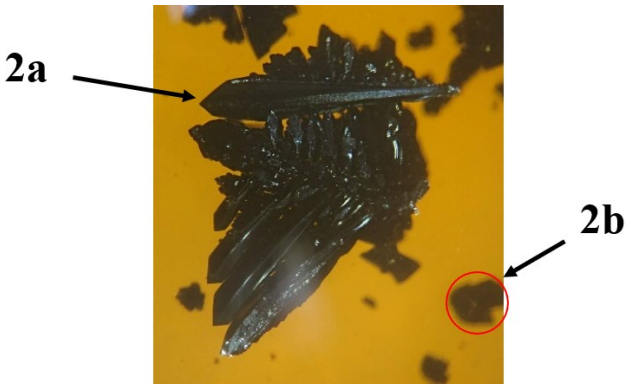

Figure S2. Image of the single crystals for **2a** and **2b**.

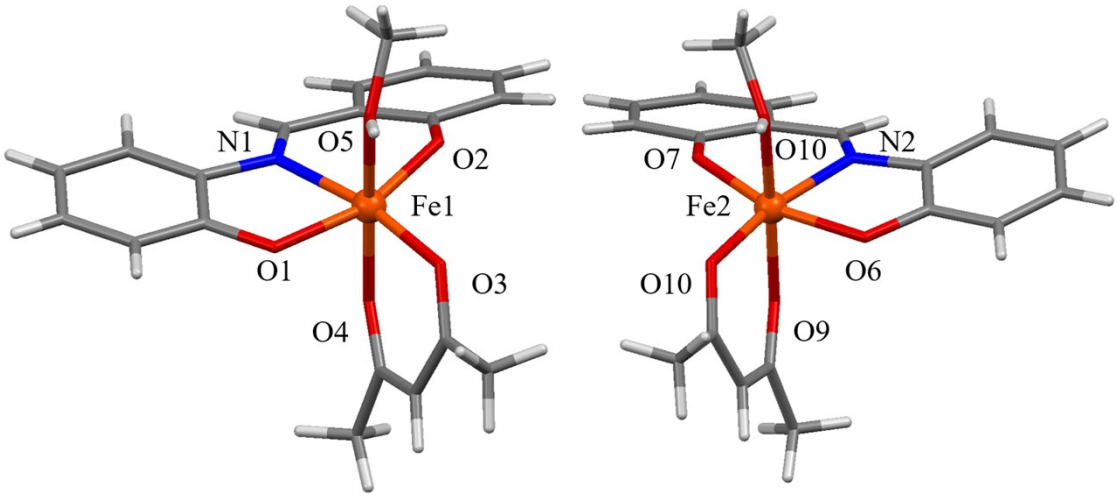

Figure S3. Each asymmetric crystal structures (Δ, Λ) for **1** at 123 K with the atom-numbering scheme.

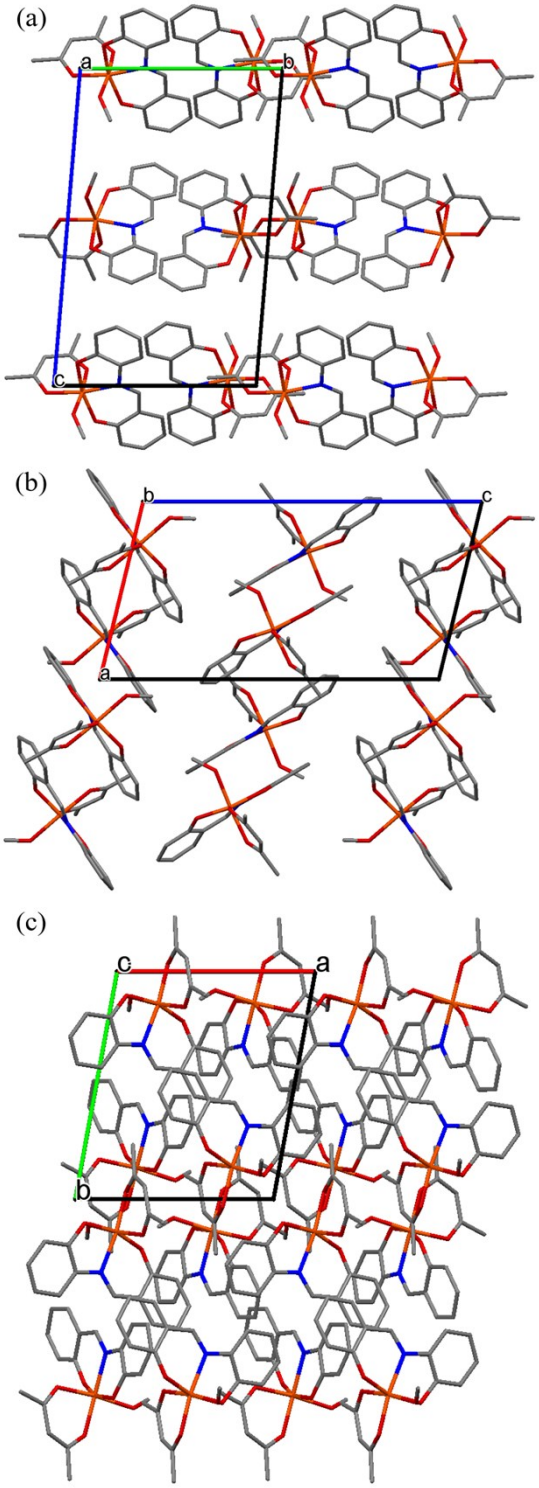

Figure S4. Crystal packing structures for **1** at 123 K along (a) *a*, (b) *b*, (c) *c* axes. Hydrogen atoms are omitted for clarity.

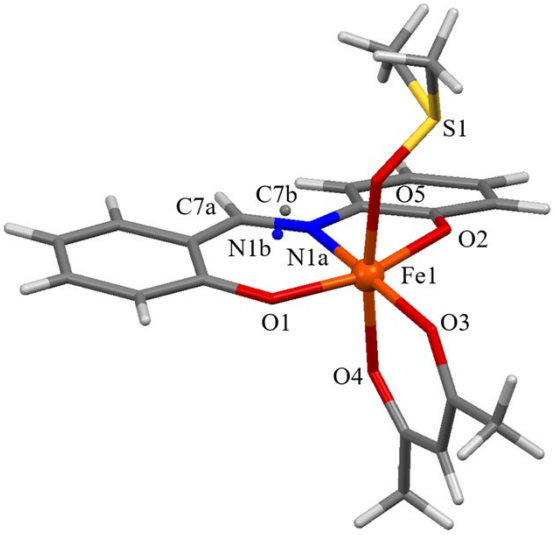

Figure S5. Crystal structure of **2a** at 298 K with the atom-numbering scheme. Disordered atoms (C7, N1) are accordance with each Δ and Λ form.

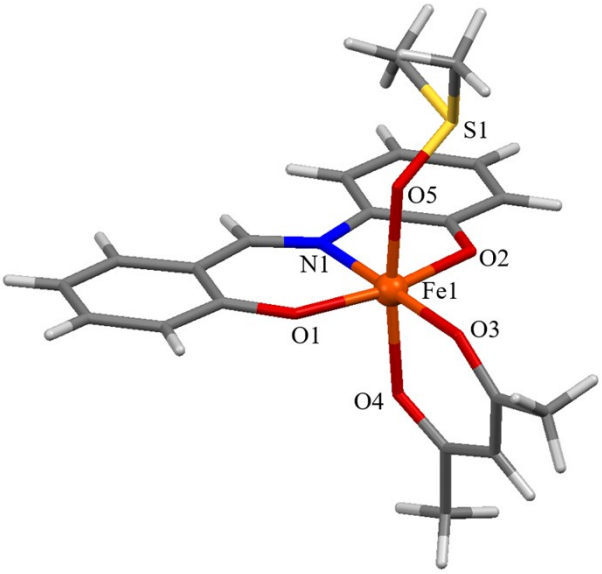

Figure S6. Crystal structure of **2b** at 298 K with the atom-numbering scheme.

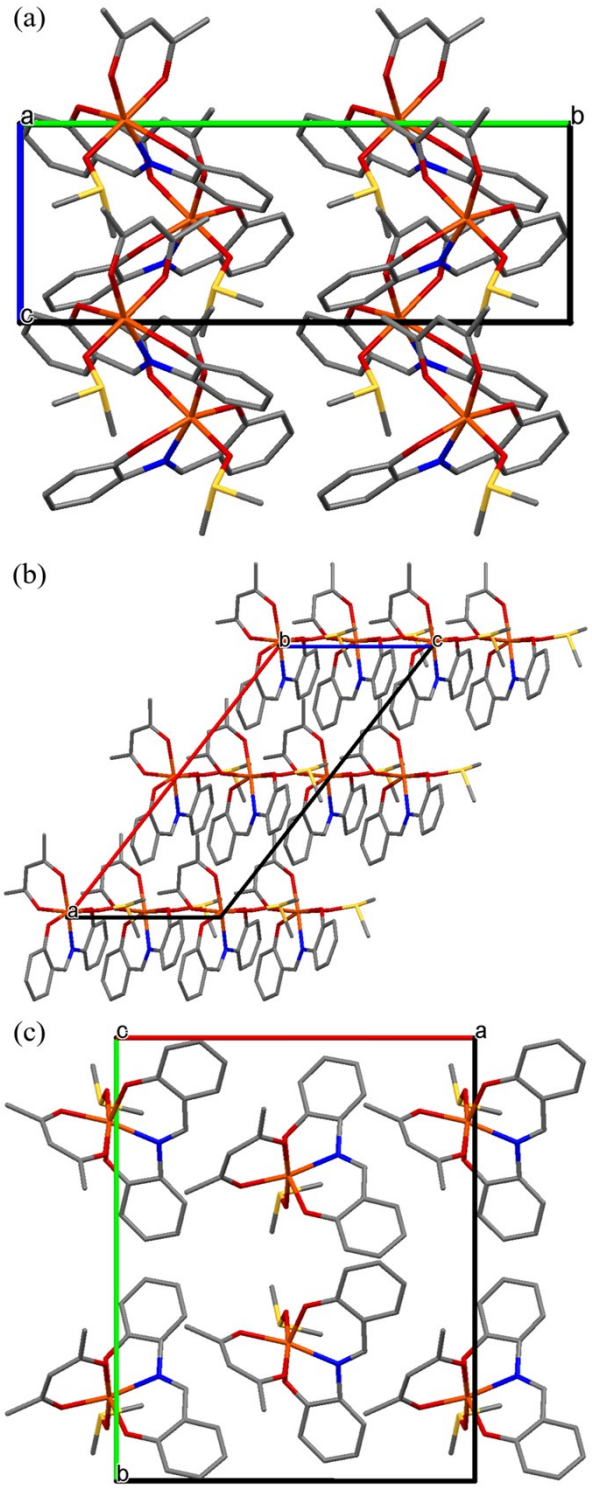

Figure S7. Crystal packing structures of **2a** at 298 K along (a) *a*, (b) *b*, (c) *c* axis. Hydrogen atoms and disordered atoms are omitted for clarity.

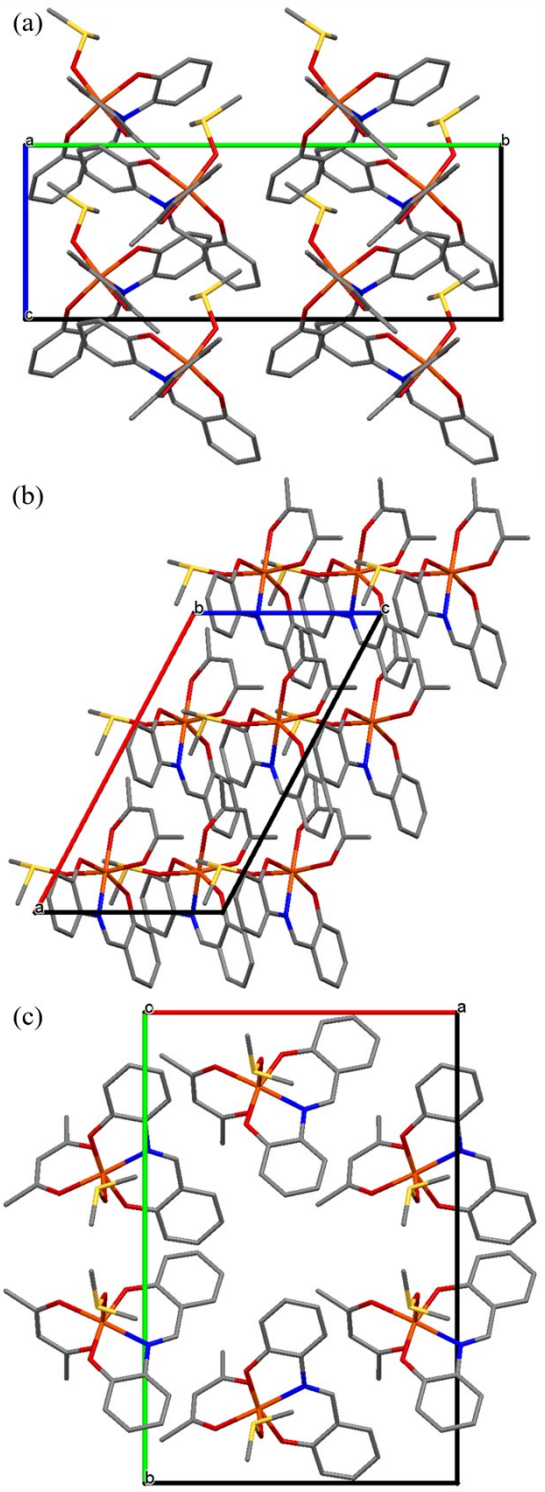

Figure S8. Crystal packing structures of **2b** at 298 K along (a) *a*, (b) *b*, (c) *c* axis. Hydrogen atoms are omitted for clarity.

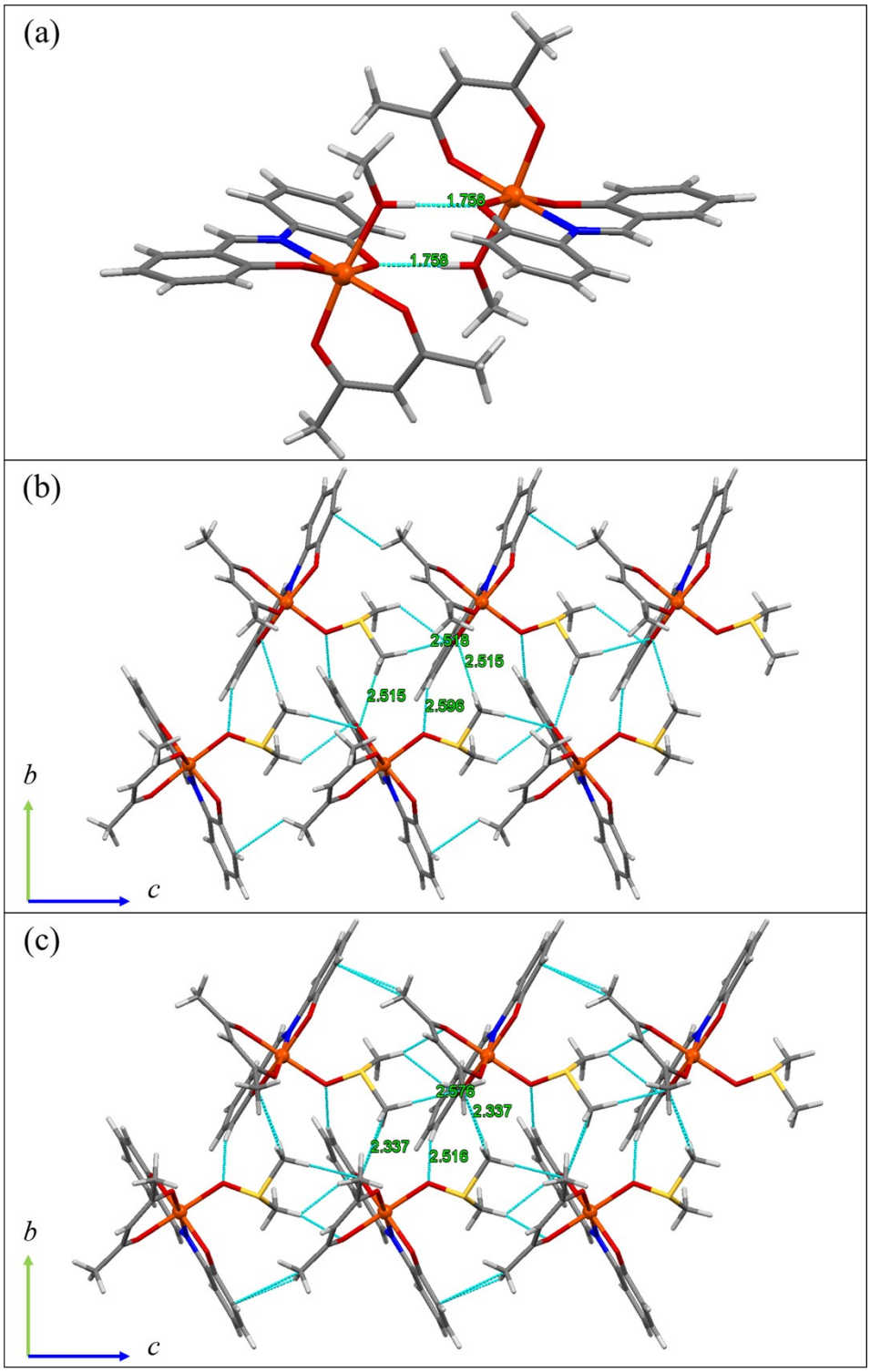

Figure S9. Intermolecular interactions of (a) **1**, (b) **2a** and (c) **2b**.

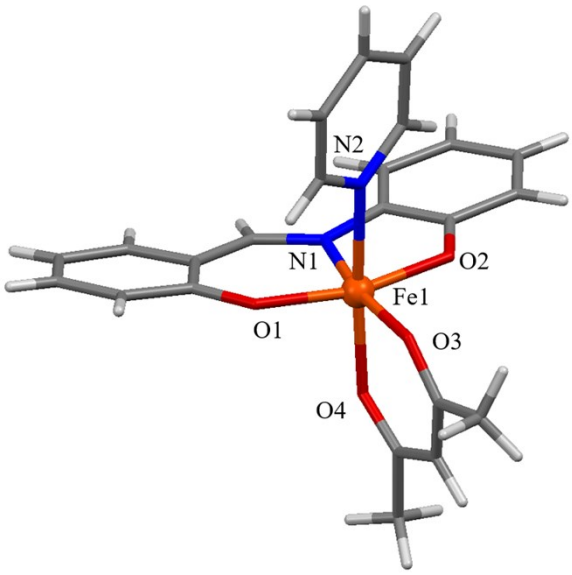

Figure S10. Crystal structure of **3** at 298 K with the atom-numbering scheme. Solvent molecules and disordered atoms are omitted for clarity.

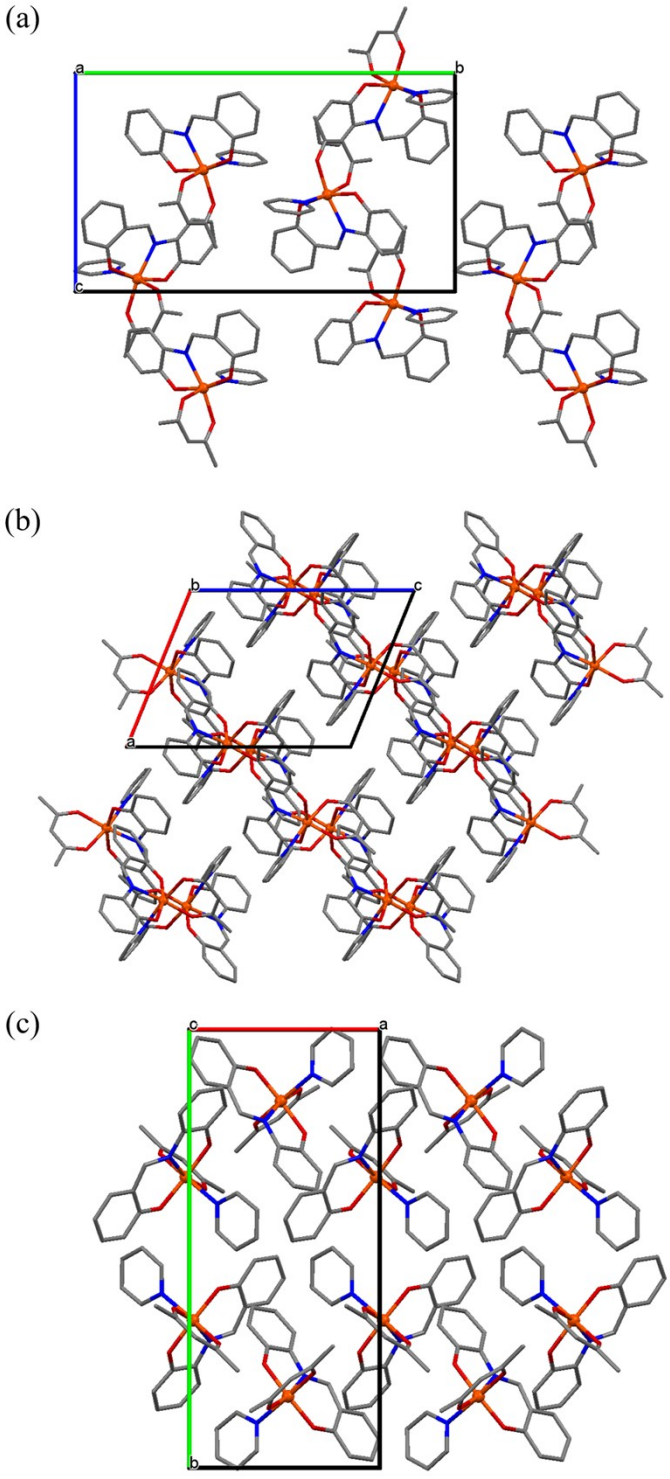

Figure S11. Crystal packing structures of **3** at 298 K along (a) *a*, (b) *b*, (c) *c* axis. Hydrogen atoms, solvent molecules and disordered atoms are omitted for clarity.

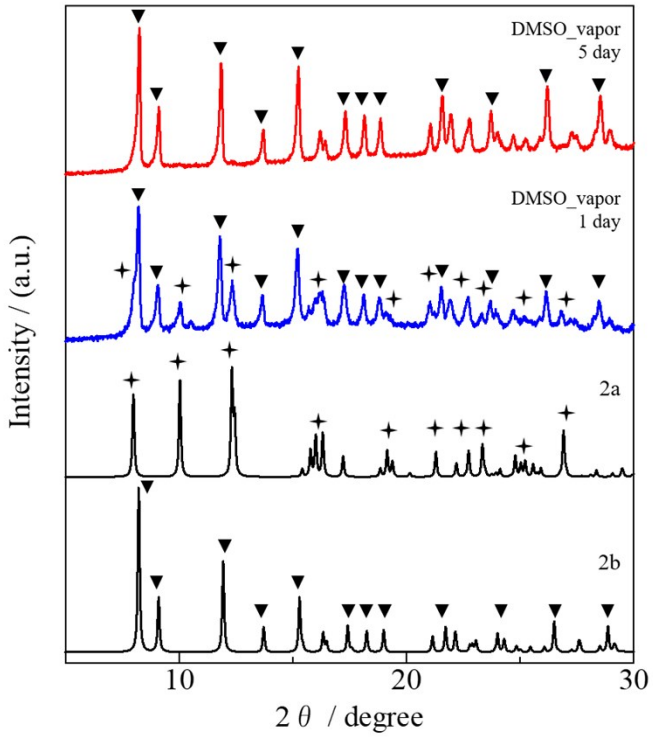

Figure S12. Time dependence of PXRD patterns for DMSO-vapor exposed **1** at room temperature.

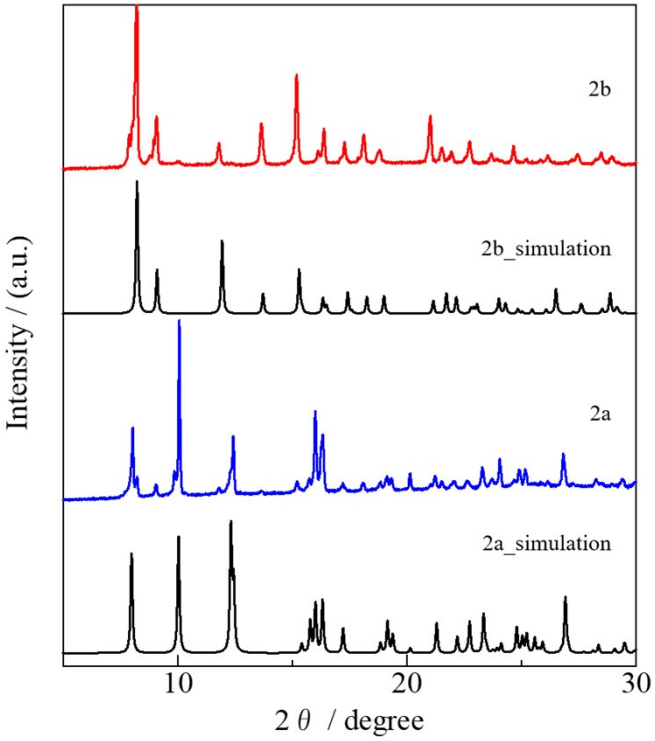

Figure S13. PXRD patterns for the crystalline samples of **2a** and **2b** at room temperature and their simulations.

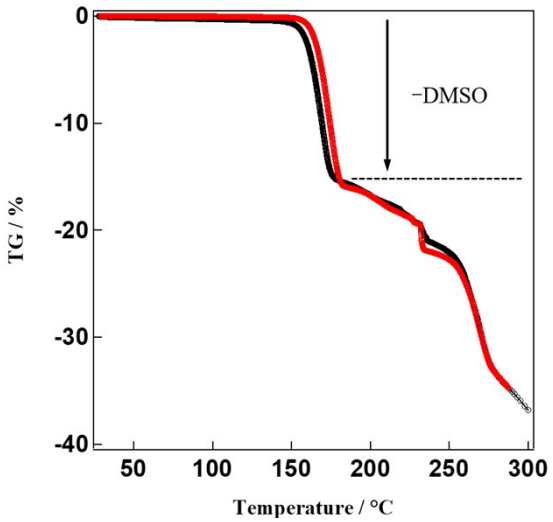

Figure S14. TGA curves for **2a** (black) and **2b** (red).

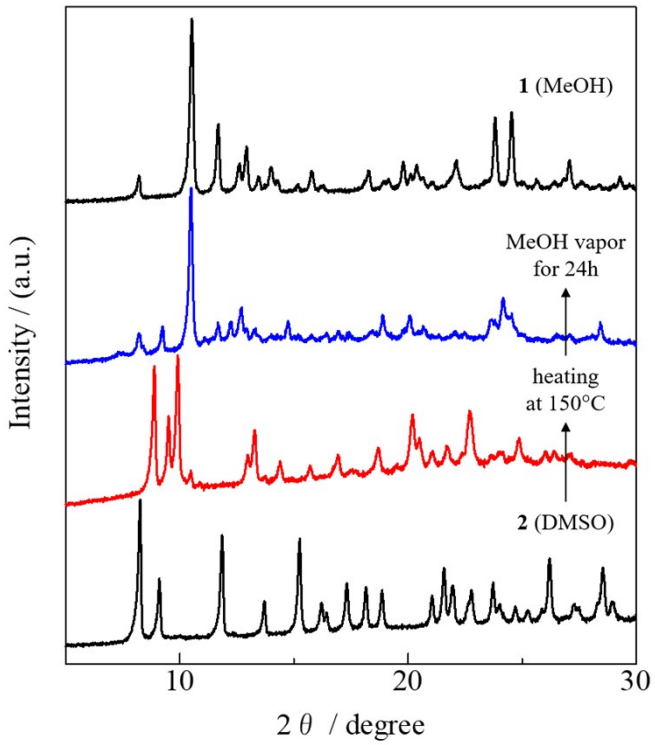

Figure S15. PXRD patterns for the desolvated **2** and MeOH-vapor exposed samples.

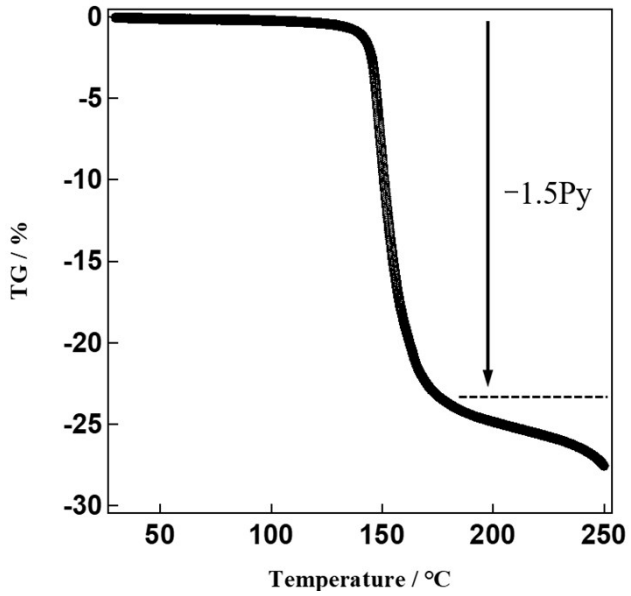

Figure S16. TGA curve for **3**. 24% weight loss was observed above ca. 160°C. This shows good agreement with the pyridine content of **3** (1.5py = 24.5%).

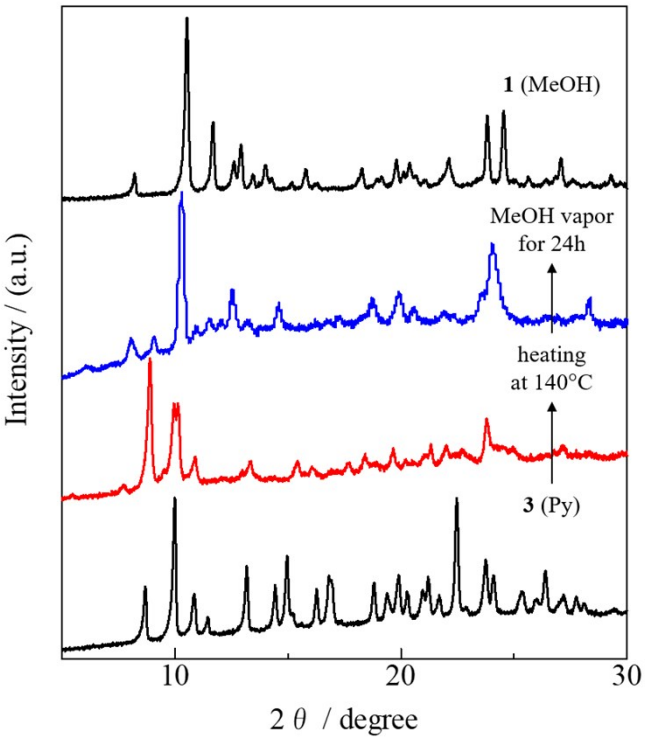

Figure S17. PXRD patterns for the desolvated **3** and MeOH-vapor exposed samples. Following the initial thermal treatment of crystalline **3** at 140°C for 1 h under reduced pressure to remove the pyridine, the PXRD pattern of the desolvated sample, following its exposure to MeOH vapor, was again measured.

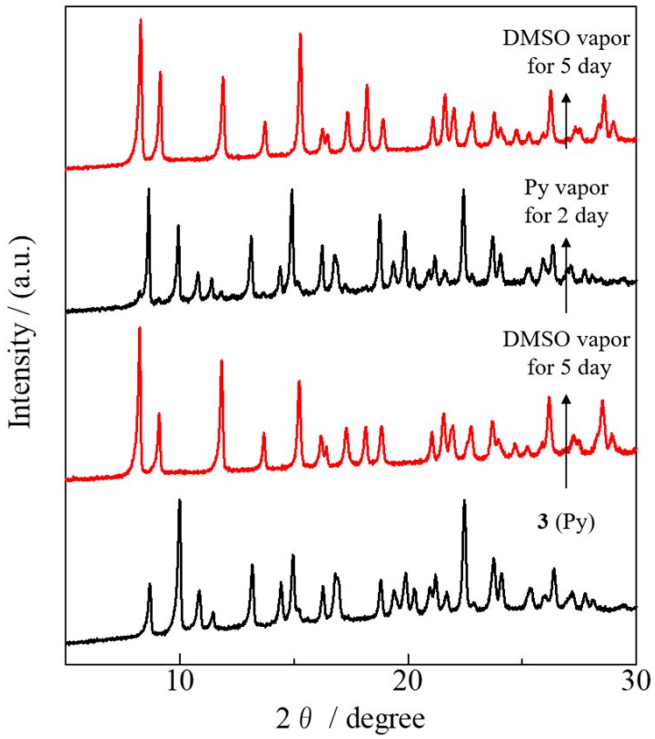

Figure S18. PXRD patterns for **3** after exposure to DMSO vapor (red) and **2** after exposure to pyridine vapor (black).

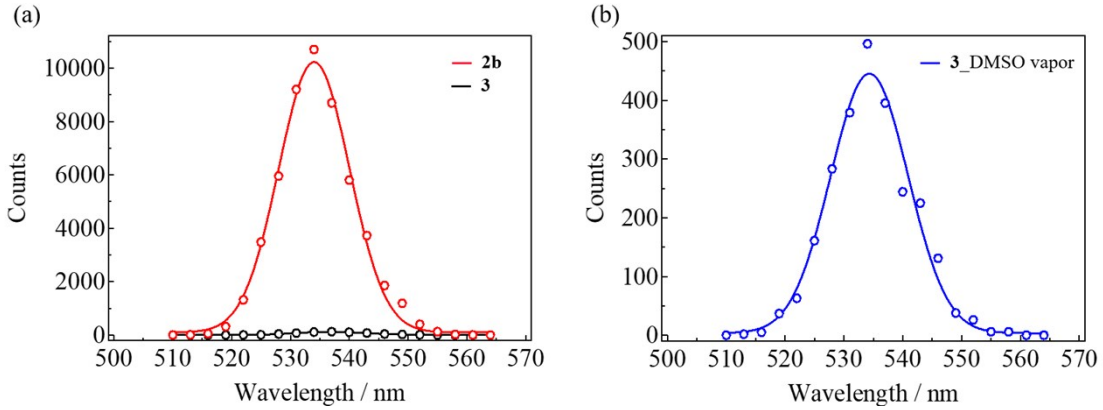

Figure S19. Results of SHG experiments for (a) **2b**, **3** and (b) **3** after exposing to DMSO vapor.

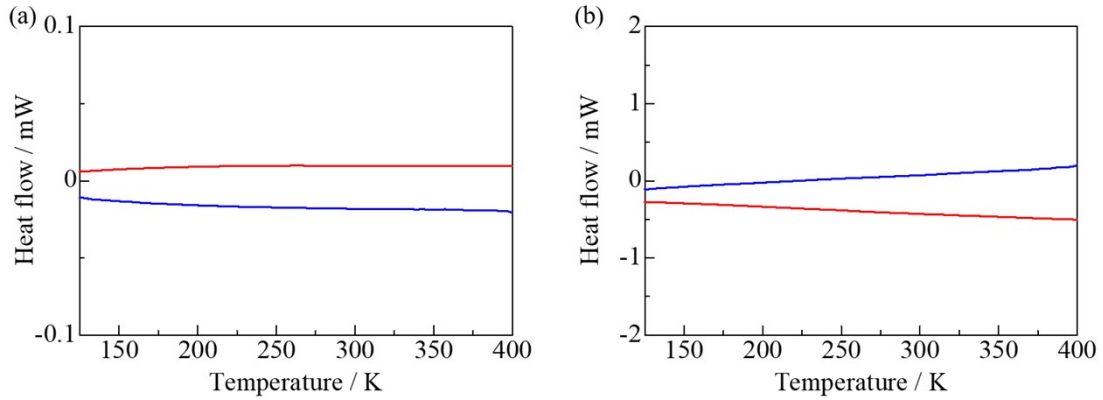

Figure S20. DSC curves for (a) **2a** and (b) **2b** in the temperature range 125–400 K.

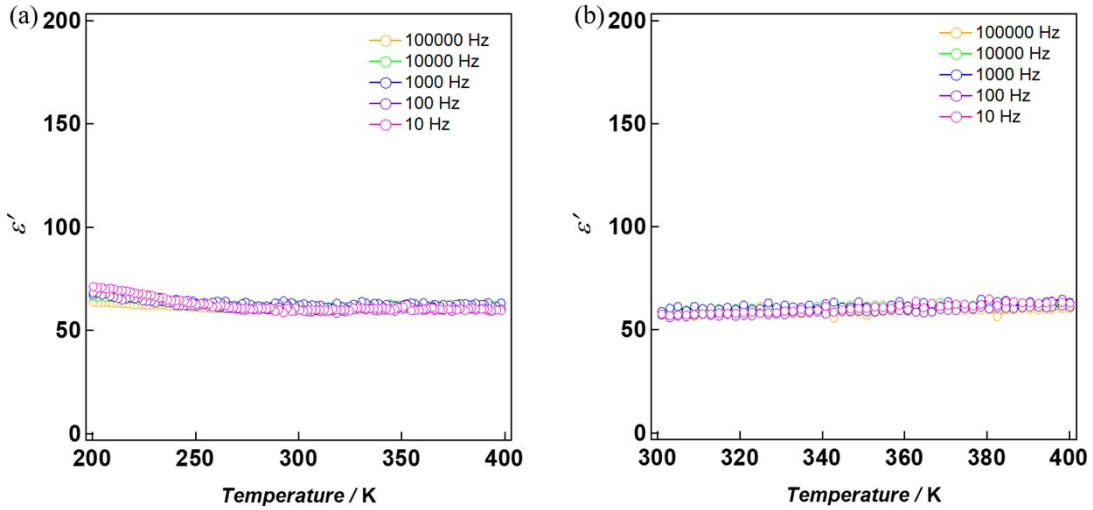

Figure S21. Temperature-dependent ε' at ac frequencies of 10–100000 Hz for a single crystal sample of (a) **2a** and (b) **2b** in the temperature range 300–400 K.

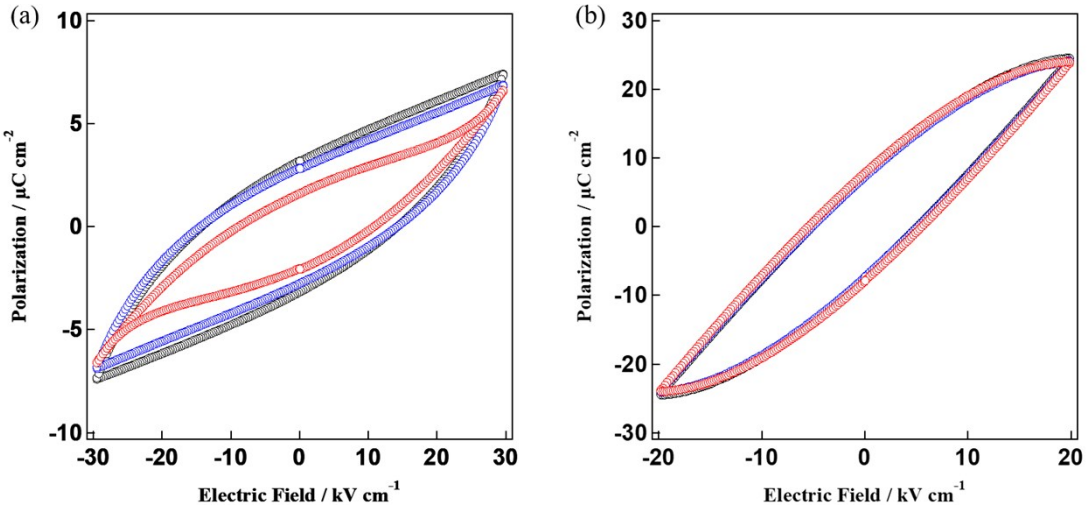

Figure S22. Temperature dependence of *P*–*E* hysteresis loops for (a) **2a** and (b) **2b** with an $E \perp C$-axis at 0.1 Hz (black: 298 K, blue: 350 K, red: 400 K).